Low-energy isovector and isoscalar dipole response in neutron-rich nuclei

D. Vretenar,[1] Y. F. Niu,[1,2] N. Paar,[1] and J. Meng[2,3,4]

[1]*Department of Physics, Faculty of Science, University of Zagreb, Croatia*

[2]*State Key Laboratory for Nuclear Physics and Technology, School of Physics, Peking University, Beijing 100871, China*

[3]*School of Physics and Nuclear Energy Engineering, Beihang University, Beijing 100191, China*

[4]*Department of Physics, University of Stellenbosch, Stellenbosch 7602, South Africa*

(Received 24 February 2012; revised manuscript received 2 April 2012; published 17 April 2012)

The self-consistent random-phase approximation, based on the framework of relativistic energy density functionals, is employed in the study of isovector and isoscalar dipole response in ^{68}Ni, ^{132}Sn, and ^{208}Pb. The evolution of pygmy dipole states (PDSs) in the region of low excitation energies is analyzed as a function of the density dependence of the symmetry energy for a set of relativistic effective interactions. The occurrence of PDSs is predicted in the response to both the isovector and the isoscalar dipole operators, and its strength is enhanced with the increase in the symmetry energy at saturation and the slope of the symmetry energy. In both channels, the PDS exhausts a relatively small fraction of the energy-weighted sum rule but a much larger percentage of the inverse energy-weighted sum rule. For the isovector dipole operator, the reduced transition probability $B(E1)$ of the PDSs is generally small because of pronounced cancellation of neutron and proton partial contributions. The isoscalar-reduced transition amplitude is predominantly determined by neutron particle-hole configurations, most of which add coherently, and this results in a collective response of the PDSs to the isoscalar dipole operator.

DOI: 10.1103/PhysRevC.85.044317 PACS number(s): 21.60.Jz, 24.30.Cz, 24.30.Gd, 21.65.Ef

I. INTRODUCTION

Studies of collective excitations play a crucial role in our understanding of complex properties of nuclei. The multipole response of unstable nuclei and, in particular, a possible occurrence of new exotic modes of excitation in weakly bound nuclear systems presents a rapidly growing field of research [1,2]. During the last decade, a number of experimental studies have been performed on the low-energy electric dipole response in neutron-rich medium-heavy and heavy nuclei [3–20].

The structure and dynamics of low-energy dipole strength, also referred to as a pygmy dipole state (PDS) or resonance, has extensively been investigated using a variety of theoretical approaches and models [1]. Recent papers have made use of the Hartree-Fock (HF) plus random-phase approximation (RPA) [21–28], the self-consistent RPA based on the AV18 nucleon-nucleon interaction and phenomenological three-body contact terms [29], the Hartree-Fock-Bogoliubov model plus quasiparticle (Q)RPA [30–36], quasiparticle RPA plus phonon coupling [37], the quasiparticle-phonon model [38], the quasiparticle-phonon model including complex configurations of up to three phonons [12,17,18], the second RPA [39], the relativistic RPA [40–43] and QRPA [44–47], the relativistic quasiparticle time-blocking approximation [48–51], and the semiclassical Landau-Vlasov approach [52,53].

In addition to the fact that pygmy states present an intrinsically interesting structure phenomenon in neutron-rich nuclei, it has been suggested that they might constrain the radius of the neutron distribution in medium-heavy and heavy nuclei [9] and may provide information about the density dependence of the symmetry energy [40]. Prompted by recent experiments that have reported accurate data on the distribution of PDSs in medium-heavy nuclei [6–18] and by the model-independent determination of the neutron-skin thickness in ^{208}Pb with parity-violating elastic electron scattering [54], in the past two years, several theoretical papers have explored the relation among the PDSs, the density dependence of the symmetry energy, and the neutron skin [23,24,28,43]. These papers are based on the microscopic framework of nuclear energy density functionals plus the QRPA.

Starting from a representative set of Skyrme effective forces and meson-exchange effective Lagrangians, Carbone *et al*. [23] performed an RPA analysis of the correlation among the density dependence of the nuclear symmetry energy, the neutron skin, and the percentage of energy-weighted sum rule (EWSR) exhausted by the PDSs in ^{68}Ni and ^{132}Sn. In comparison with available data, it was possible to constrain the value of the derivative of the symmetry energy at saturation and to use this constraint to determine the neutron-skin radii of ^{68}Ni, ^{132}Sn, and ^{208}Pb. In contrast to this result, Reinhard and Nazarewicz [24], by using the covariance analysis to identify observables and pseudo-observables that correlate with the neutron skin, suggested that the neutron skin of ^{208}Pb was strongly correlated with the dipole polarizability but very weakly correlated with the low-energy electric dipole strength. This finding has recently been challenged by Piekarewicz [43] in an analysis of the distribution of electric dipole strength in ^{68}Ni by using a relativistic RPA with a set of effective interactions that predict significantly different values for the neutron-skin thickness of ^{208}Pb. The results not only suggest a strong correlation between the dipole polarizability of ^{68}Ni and the neutron-skin thickness of ^{208}Pb, but also a correlation just as strong between the neutron-skin thickness of ^{208}Pb and the fraction of the dipole polarizability exhausted by the pygmy dipole strength. In a very recent study performed by using the self-consistent Skyrme HF plus RPA approach, Roca-Maza *et al*. [28] have analyzed the isospin character, the degree of collectivity, and the sensitivity to the slope of the nuclear symmetry energy of the low-energy dipole response in

^{68}Ni, ^{132}Sn, and ^{208}Pb. It has been shown that both the isoscalar and the isovector strength functions display a low-energy peak that is enhanced and is shifted to higher excitation energies with increasing values in the slope of the symmetry energy at saturation. The degree of collectivity associated with the RPA state(s) that contribute to this peak differs in the isoscalar and isovector channels. Much more collectivity in the PDS is predicted in the response to the isoscalar dipole operator.

In this paper, we perform an analysis similar to that of Ref. [28] but by using a more systematic set of effective nuclear interactions. Namely, to analyze the model dependence of the predicted PDS, Roca-Maza *et al*. employed three different Skyrme parameter sets: SGII, SLy5, and SkI3. These interactions span a broad range of values of the slope of the nuclear symmetry energy at saturation, but they also differ in other characteristics in a nonsystematic way. A consistent set of effective interactions was used by Piekarewicz in Ref. [43] to analyze the distribution of the PDS but only for ^{68}Ni and only in the isovector channel.

II. THEORETICAL FRAMEWORK

The present analysis employs the fully self-consistent relativistic random-phase approximation (RRPA) based on the framework of relativistic energy density functionals [55]. In the relativistic mean-field (RMF) + RPA model, effective interactions are implemented in a fully consistent way: Effective Lagrangians with density-dependent meson-nucleon couplings are employed [56,57], and the same interactions are used both in the RMF equations that determine the ground state and in the matrix equations of the RRPA. The full set of RRPA equations is solved by diagonalization. The results are excitation energies E_λ and the corresponding forward- and backward-going amplitudes X^λ and Y^λ, respectively, that are used to evaluate the reduced transition probability from an excited state $|J\lambda\rangle$ to the ground state,

$$B^T(EJ) = \frac{1}{2J_i+1}\left|\sum_{\mu\mu'}\left\{X^{\lambda,J}_{\mu\mu'}\langle\mu\|\hat{Q}^T_J\|\mu'\rangle + (-1)^{j_\mu - j_{\mu'}+J}Y^{\lambda,J}_{\mu\mu'}\langle\mu'\|\hat{Q}^T_J\|\mu\rangle\right\}\right|^2, \quad (1)$$

where μ and μ' denote single-nucleon states. Discrete spectra are averaged with a Lorentzian distribution of arbitrary width (1.5 MeV in the present paper). The electric $E1$ response is calculated for the isovector dipole operator,

$$\hat{Q}^{T=1}_{1\mu} = \frac{N}{N+Z}\sum_{p=1}^{Z} r_p Y_{1\mu}(\hat{r}_p) - \frac{Z}{N+Z}\sum_{n=1}^{N} r_n Y_{1\mu}(\hat{r}_n), \quad (2)$$

and the isoscalar dipole operator,

$$\hat{Q}^{T=0}_{1\mu} = \sum_{i=1}^{A} r_i^3 Y_{1\mu}(\hat{r}_i) - \eta\sum_{i=1}^{A} r_i Y_{1\mu}(\hat{r}_i). \quad (3)$$

The inclusion of the second term in the isoscalar operator Eq. (3) with $\eta = 5\langle r^2\rangle/3$ ensures that the corresponding strength distribution does not contain spurious components associated with the center-of-mass motion [58]. The strength function reads

$$S(E) = \sum_\nu \left|\langle\nu\|\hat{Q}^T_J\|0\rangle\right|^2\delta(E-E_\nu). \quad (4)$$

E_ν is the energy of the RPA state $|\nu\rangle$, and the moments of the strength distribution are defined as

$$m_k = \int dE\, E^k S(E) = \sum_\nu E^k_\nu\left|\langle\nu\|\hat{Q}^T_J\|0\rangle\right|^2. \quad (5)$$

In the following, we analyze the occurrence and structure of the PDSs in the isovector and isoscalar dipole responses of ^{68}Ni, ^{132}Sn, and ^{208}Pb in relation to the density dependence of the symmetry energy. In linear order with respect to the nuclear matter density ρ, the symmetry energy $S(\rho)$ is determined by its value at saturation density $S(\rho_0) \equiv a_4$ and by the derivative at saturation density,

$$S'(\rho)|_{\rho=\rho_0} \equiv \frac{L}{3\rho_0}, \quad (6)$$

and this relation defines the "slope" parameter L. By using data on the percentage of the EWSR associated with the PDSs in ^{68}Ni [15] and ^{132}Sn [9], Carbone *et al*. [23] constrained the value of the slope parameter $L = 64.8 \pm 15.7$MeV in accordance with values previously determined with different types of analyses and/or other methods based on nuclear structure and heavy-ion experiments. Here, we employ the framework of relativistic energy density functionals represented by effective Lagrangians with density-dependent meson-nucleon vertex functions. The parameters of the very successful effective interactions DD-ME1 [56] and DD-ME2 [57], in particular, were adjusted simultaneously to empirical properties of symmetric and asymmetric nuclear matter and to binding energies and charge radii of 12 spherical nuclei. Data on excitation energies of isoscalar (IS) giant monopole resonances and isovector dipole giant resonances (IVGDRs) were also used to determine the compressibility modulus and asymmetry energy at saturation as well as available data on differences between neutron and proton radii in Sn isotopes and ^{208}Pb. Numerous calculations have shown that these interactions provide accurate results for ground-state properties of spherical and deformed nuclei as well as excitation energies of giant resonances. Pertinent to the present analysis, the RRPA with the DD-ME2 effective interaction predicts the dipole polarizability,

$$\alpha_D = \frac{8\pi}{9}e^2 m_{-1} \quad (7)$$

(directly proportional to the inverse energy-weighted moment m_{-1}) for ^{208}Pb: 20.8 fm^3 in very good agreement with the recently measured value $\alpha_D = (20.1 \pm 0.6)$ fm^3 [20].

III. RESULTS

In an earlier paper [59], we used the RRPA with density-dependent meson-nucleon effective interactions to provide a microscopic estimate of the nuclear matter compressibility and symmetry energy in relativistic mean-field models. Starting

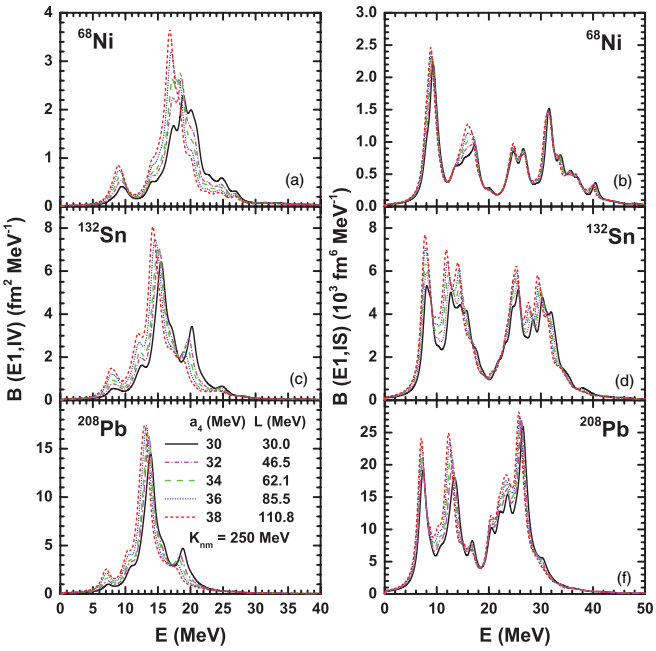

FIG. 1. (Color online) The RRPA isovector (left column) and isoscalar (right column) dipole strength distributions in ^{68}Ni, ^{132}Sn, and ^{208}Pb, calculated with a set of five effective interactions that differ in the value of the symmetry energy at saturation (a_4) and the corresponding slope parameter L.

from the parametrization DD-ME1 [56], three families of interactions with nuclear matter incompressibility $K_{\rm nm} = 230$, 250, and 270 MeV were constructed. For each value of $K_{\rm nm}$, five interactions were adjusted with $a_4 = 30$, 32, 34, 36 and 38 MeV, respectively. For particular values of $K_{\rm nm}$ and a_4, the remaining parameters of these interactions were fine-tuned to empirical properties of nuclear matter and to the binding energies and charge radii of ten spherical nuclei. It was noted that, to reproduce the empirical masses of $N \neq Z$ nuclei, larger values of a_4 necessitate an increase in the slope parameter L of the symmetry energy. These effective interactions were used in Ref. [9] to study a possible correlation between the observed PDS in ^{130,132}Sn and the corresponding values for the neutron-skin thickness. In addition to DD-ME2 ($K_{\rm nm} = 251$ MeV), the set of effective interactions with $K_{\rm nm} = 250$ MeV and $a_4 = 30$, 32, 34, 36 and 38 MeV will here be used to study the PDS in the isovector and isoscalar dipole responses of spherical closed-shell nuclei.

For this set of effective interactions, in Fig. 1, we display the total IV and IS RRPA dipole strength functions for ^{68}Ni, ^{132}Sn, and ^{208}Pb. The IV dipole response in all three nuclei is, of course, dominated by the collective GDR peaked in the high-energy region around 15 MeV. As already shown in Refs. [55,60], as a result of the increase in L with a_4, the excitation energy of the IVGDR decreases with increasing $S(\rho_0) \equiv a_4$ because this increase implies a reduction in the symmetry energy at low densities, characteristic for surface modes. In addition, one notices an enhancement of $E1$ strength in the low-energy region below 10 MeV. This PDS is very sensitive to the density dependence of the symmetry energy and is strongly enhanced by the increase in L and a_4. The same pygmy states are also present in the IS strength functions, and this is clear evidence of the mixed isovector-isoscalar nature of the PDS. The isoscalar $E1$ strength distributions display a characteristic bimodal structure with two broad components: one in the low-energy region close to the IVGDR ($\approx 2\hbar\omega$) and the other at higher energy close to the electric octupole resonance ($\approx 3\hbar\omega$). Theoretical analyses have shown that the high-energy component represents compressional vibrations [58,61,62]. The high-energy ISGDR is a second-order effect, built on $3\hbar\omega$ or higher configurations, and corresponds to a compression wave traveling back and forth through the nucleus along a definite direction. Some states, which comprise the broad structure in the low-energy region, correspond to vortical nuclear flow associated with the toroidal dipole moment [52,63–65]. However, as pointed out in a paper on the interplay between compressional and vortical nuclear currents [64], a strong mixing between compressional and vorticity vibrations in the isoscalar $E1$ states can be expected up to the highest excitation energies in the region of $\approx 3\hbar\omega$. Finally, the lowest peaks in the isoscalar strength functions are associated with the PDS. A very interesting result is that, relative to the corresponding GDR, the PDS is much more pronounced in the isoscalar channel. In fact, for ^{68}Ni, the pygmy state has the largest $B(E1)$ value among the isoscalar states, and the IS strength function, except for the structure around 15 MeV, is not sensitive to the variation in the density dependence of the symmetry energy. One expects more isospin mixing in the two heavier nuclei (see also the analysis of Ref. [45]), and this is reflected in the enhancement of the $B(E1)$ values with the increase in L and a_4 for all states in the response of ^{132}Sn and ^{208}Pb to the isoscalar dipole operator Eq. (3). This enhancement is more pronounced below the ISGDR, that is, in the region around 15 MeV where one expects mixing with the IVGDR and for the PDS.

Even though the set of effective interactions that we use here spans a relatively broad interval of values of the parameters a_4 and L that characterize the density dependence of the symmetry energy, the effect on the excitation energy of the IVGDR is not large, especially in a heavy nucleus, such as ^{208}Pb. In fact, as shown in Fig. 1, the IVGDR peak energy in ^{208}Pb is lowered by less than 1 MeV in the interval between $a_4 = 30$, $L = 30$MeV and $a_4 = 38$, $L = 111$ MeV. A better distinction between these effective interactions is obtained by considering predicted values for the electric dipole polarizability of ^{208}Pb [cf. Eq. (7)] in comparison with the experimental value $\alpha_D = (20.1 \pm 0.6)\,{\rm fm}^3$ [20]. The results are shown in Fig. 2. In addition to the values obtained with the five effective interactions $a_4 = 30$, 32, 34, 36, and 38 MeV, we also include the polarizability calculated with the interaction DD-ME2 ($a_4 = 32.3$ and $L = 51.5$ MeV) that was adjusted independently in Ref. [57]. The result closest to the experimental value corresponds to the effective interaction with $a_4 = 32$ and $L = 46.5$ MeV and the value predicted by DD-ME2: $\alpha_D = 20.8$ MeV is just 100 keV outside the experimental error bar. The slope parameters of these two interactions are slightly below the value $L = 64.8 \pm 15.7$ MeV that Carbone *et al.* [23] deduced from the percentage of the EWSR associated with the PDSs in ^{68}Ni [15] and ^{132}Sn [9]. From Fig. 2, it is apparent that only the values of α_D predicted

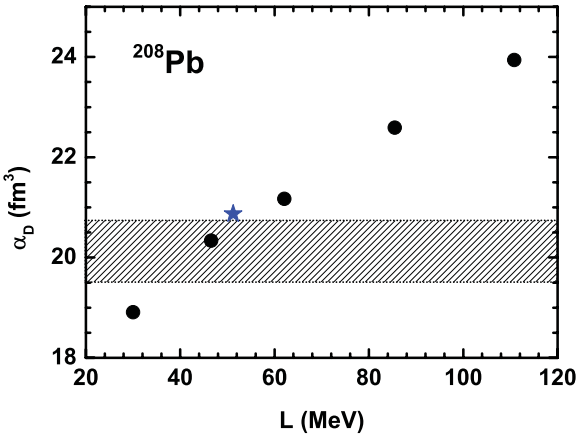

FIG. 2. (Color online) Predictions for the electric dipole polarizability Eq. (7) of ^{208}Pb, calculated with a set of five effective interactions that differ in the value of the symmetry energy at saturation (a_4) and the corresponding slope parameter L (circles), and the effective interaction DD-ME2 (star) [57]. The shaded area delineates the experimental constraint $\alpha_D = (20.1 \pm 0.6)\text{fm}^3$ [20].

by the two interactions with $a_4 = 36$, $L = 85.5$ MeV and $a_4 = 38$, $L = 110.8$ MeV are in serious disagreement with the experiment.

For ^{68}Ni in Fig. 3, we display the moments of the dipole strength distributions m_0, m_1, and m_{-1} for the isovector [panels (a)–(f)] and isoscalar [panels (g)–(i)] channels. $E = 12$ MeV is the model-dependent, although obvious, choice for the excitation energy that separates the low-energy PDS region from the energy interval dominated by the collective giant resonance (cf. Fig. 1). In the left column, we plot the absolute values of the moments of the isovector and isoscalar strength distributions in the PDS region, whereas, the column on the right displays the percentages of the total moment exhausted in the PDS interval as a function of the slope parameter L of the six effective interactions used in the present paper. The shaded area denotes the experimental result and the corresponding uncertainty of the percentage of EWSR associated with the PDS in ^{68}Ni [15,23]. We note that the absolute values of moments in the low-energy region, as well as the percentages of the total moment exhausted in the PDS interval, increase linearly with the slope of the symmetry energy. In both the isovector and the isoscalar channels, the smallest percentage exhausted by the PDS is for the m_1 moment. This is because m_1 is energy weighted and, therefore, is dominated by the main giant-resonance structure in the high-energy region. Much more sensitive to the PDS is the moment m_{-1}, directly proportional to the total polarizability Eq. (7) because the inverse energy weighting enhances the low-energy part of the response. In the isovector channel, in particular, the percentage of the total polarizability exhausted by the PDS is more than three times the percentage of the EWSR exhausted by the low-energy pygmy strength. These results are in agreement with those reported by Piekarewicz [43], obtained using a different class of relativistic effective interactions but with a similar range of values for the slope parameter of the symmetry energy. What is different here are the results for the moments of the isoscalar strength distributions shown in the lower panel

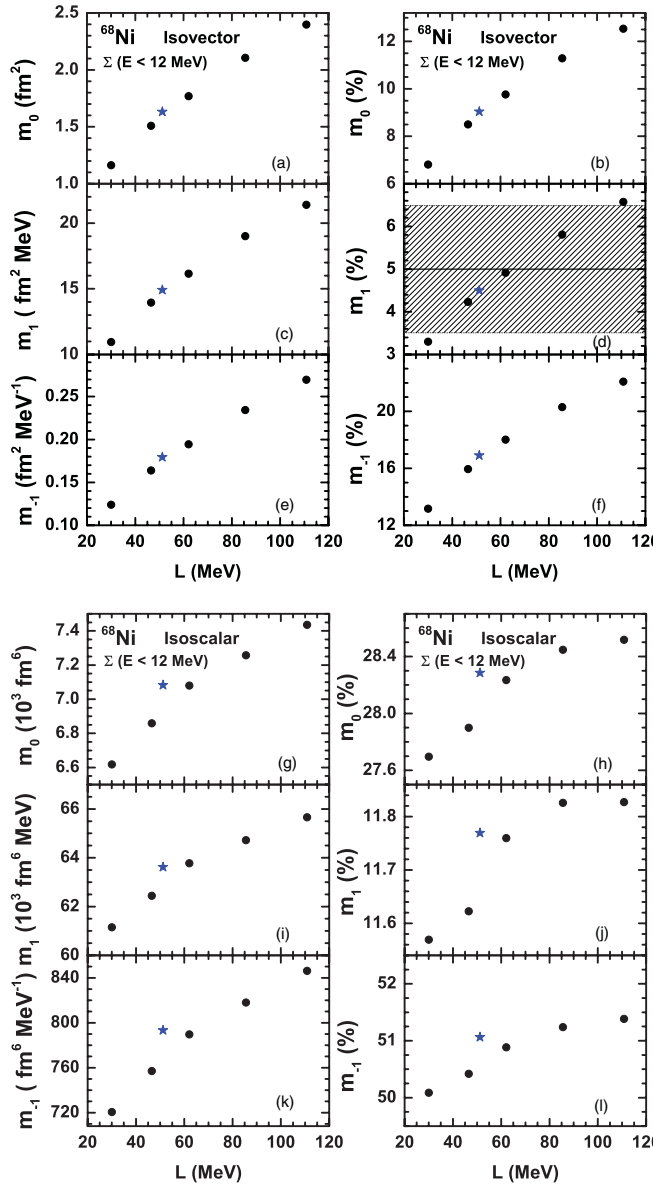

FIG. 3. (Color online) Moments m_0, m_1, and m_{-1} of the isovector [panels (a)–(f)] and isoscalar [panels (g)–(i)] dipole strength distributions of ^{68}Ni. Absolute values of the moments in the low-energy PDS region below $E < 12$ MeV (left column) and the percentages of the total moments exhausted by the PDS (right column) as a function of the slope parameter L of the six effective interactions used in this paper.

of Fig. 3. In this case, the PDS exhausts more than 10% of the EWSR and more than 50% of the m_{-1} moment for all values of the slope parameter L. Similar results are also found for the moments of the isovector and isoscalar dipole strength distributions of ^{132}Sn and ^{208}Pb.

An important issue is the degree of collectivity of the PDS. In most of the early theoretical papers, the measure of collectivity was associated with the number of particle-hole configurations that significantly contribute to the RPA amplitude of the principal pygmy state. Such a measure, however, does not take into account the coherence of these

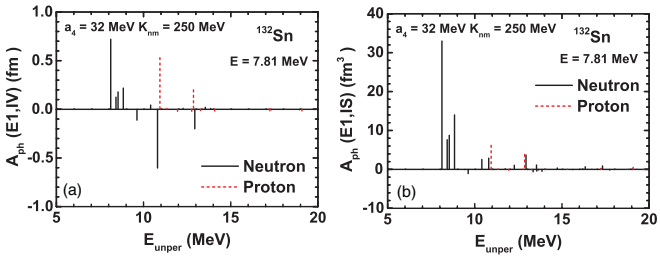

FIG. 4. (Color online) Partial contributions of neutron and proton configurations to the isovector- (left) and isoscalar- (right) reduced transition amplitude of the PDS state at 7.81-MeV excitation energy in ^{132}Sn for the effective interaction with $a_4 = 32$ and $K_{\rm nm} = 250$ MeV as functions of the unperturbed energy of the particle-hole configurations. Only amplitudes with a magnitude larger than $\approx$0.01fm (isovector) and ≈ 0.1 fm^3 (isoscalar) are shown in the figure.

contributions. Lanza *et al.* [22] analyzed the collectivity of the PDS by considering the partial contributions to the reduced transition amplitude. Namely, the reduced transition probability Eq. (1) from the ground state to the excited state $|J\lambda\rangle$ can be written as

$$B^T(EJ) = \left| \sum_{\rm ph} A_{\rm ph}^{T\lambda}(EJ) \right|^2, \qquad (8)$$

where the summation is over all particle-hole configurations that build the excited RPA state. This expression shows that the reduced transition probability is determined by the number of configurations that contribute with a significant weight as well as by the coherency (relative sign) of these contributions. The RPA state can be considered as a resonance if the corresponding reduced transition amplitude is composed of more than just a few particle-hole partial amplitudes similar in magnitude and with the same relative sign. By comparing the contributions of the partial amplitudes $A_{\rm ph}^{T=1\lambda}(E1)$ for the pygmy state and the isovector giant dipole resonance in ^{132}Sn, Lanza *et al.* [22] concluded that, although the main pygmy state can indeed be formed by many particle-hole configurations, the reduced transition probability $B(E1)$ is generally small because the corresponding partial amplitudes cancel out to a large extent. This is in contrast to the GDR for which many configurations add coherently to build a large transition amplitude. In their paper on the low-lying dipole response in ^{68}Ni, ^{132}Sn, and ^{208}Pb, Roca-Maza *et al.* [28] have found that the isovector-reduced amplitude of the PDS is characterized by destructive interference of a relatively small number of different particle-hole configurations, and the resulting reduced transition probability does not exceed approximately two to four single-particle units. In the isoscalar channel, the largest contributions to the reduced transition amplitude predominantly arise from neutron particle-hole configurations, and most of them add coherently. This results in a collective response of the PDS to the isoscalar dipole operator, characterized by a reduced transition probability of $\approx$10–20 single-particle units.

The difference between the PDS in the isovector and isoscalar dipole responses of ^{132}Sn is illustrated in Fig. 4 where we plot the largest partial contributions of neutron and proton particle-hole configurations for the isovector- (left) and isoscalar- (right) reduced transition amplitude of the main pygmy state at 7.81-MeV excitation energy, calculated using the effective interaction with $a_4 = 32$ and $L = 46.5$ MeV. The partially reduced transition amplitudes, in units of femtometers (isovector) and fm^3 (isoscalar), are plotted as a function of the unperturbed energy of the corresponding particle-hole configurations. Only amplitudes with a magnitude larger than $\approx$0.01fm (isovector), and ≈ 0.1 fm^3 (isoscalar) are shown in the figure. About seven to eight neutron particle-hole configurations display a non-negligible partial transition amplitude, whereas, only two proton configurations contribute significantly to the isovector and isoscalar amplitudes. One notices, however, the destructive interference of proton and neutron particle-hole configurations in the isovector channel (cf. also Table I). The dominant neutron amplitudes in the PDS energy region correspond to the configurations $3s_{1/2} \rightarrow 3p_{3/2}$, $2d_{3/2} \rightarrow 3p_{1/2}$, $3s_{1/2} \rightarrow 3p_{1/2}$, and $2d_{3/2} \rightarrow 3p_{3/2}$, all with positive signs. The two large negative neutron amplitudes in the GDR region that correspond to the configurations $1h_{11/2} \rightarrow 1i_{13/2}$ and $1g_{7/2} \rightarrow 1h_{9/2}$, are almost exactly canceled by the positive proton contributions from $1g_{9/2} \rightarrow 1h_{11/2}$ and $1f_{5/2} \rightarrow 1g_{7/2}$, respectively. It is interesting to note that, as shown in Fig. 5, it is precisely the partial transition amplitudes of the latter two neutron and two proton configurations that add coherently (here with a negative sign) to produce the large collective $B(E1)$ of the IVGDR state at 15.24 MeV. The repulsive residual interaction, of course, gathers these contributions and shifts them to higher energies to build the collective GDR. Therefore, while the large proton- and neutron-reduced amplitudes in the high-energy region add coherently to build the GDR, for the PDS state at 7.81 MeV, the same particle-hole configurations with positive proton and negative neutron contributions cancel each other so that the rather small reduced transition amplitude of the PDS state is dominated by just a few neutron particle-hole configurations (note that the unperturbed PDS strength is shifted to lower energies by the residual interaction).

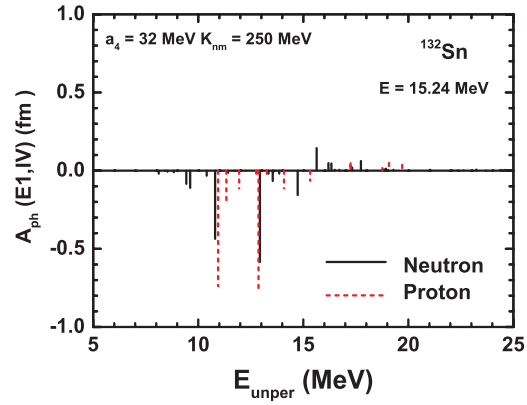

FIG. 5. (Color online) Partial contributions of neutron and proton configurations to the isovector GDR state at 15.24-MeV excitation energy in ^{132}Sn for the effective interaction with $a_4 = 32$ and $K_{\rm nm} = 250$ MeV as functions of the unperturbed energy of the particle-hole configurations. Only amplitudes with a magnitude larger than $\approx$0.01fm are shown in the figure.

TABLE I. Partial neutron and proton isovector-reduced transition amplitudes $A_{\rm ph}^{T=1}(E1)$ for the main pygmy state in ^{132}Sn. Included in the table are only amplitudes with magnitudes larger than about 0.1 fm, calculated for the five effective interactions with $a_4 = 30$, 32, 34, 36, and 38 MeV and the correspondingly increasing values of the slope parameter L. The total neutron (n) and proton (p) amplitudes are obtained by summing over all configurations also including those not listed in the table.

a_4(MeV)	Config.	30	32	34	36	38
E(MeV)		7.94	7.81	7.71	7.67	7.62
				$A_{\rm ph}^{T=1}$(fm)		
Neutron	$3s_{1/2} \rightarrow 3p_{3/2}$	0.72	0.72	0.70	0.70	0.69
	$1h_{11/2} \rightarrow 1i_{13/2}$	−0.59	−0.60	−0.60	−0.62	−0.65
	$2d_{3/2} \rightarrow 3p_{1/2}$	0.20	0.22	0.23	0.24	0.25
	$1g_{7/2} \rightarrow 1h_{9/2}$	−0.19	−0.20	−0.19	−0.20	−0.20
	$3s_{1/2} \rightarrow 3p_{1/2}$	0.18	0.17	0.16	0.16	0.16
	$2d_{3/2} \rightarrow 3p_{3/2}$	0.11	0.12	0.13	0.14	0.14
	$2d_{5/2} \rightarrow 2f_{7/2}$	−0.12	−0.11	−0.10	−0.08	−0.05
n total		0.32	0.38	0.42	0.49	0.55
Proton	$1g_{9/2} \rightarrow 1h_{11/2}$	0.49	0.53	0.55	0.60	0.66
	$1f_{5/2} \rightarrow 1g_{7/2}$	0.18	0.20	0.20	0.23	0.25
p total		0.53	0.64	0.70	0.81	0.91

The picture is very different in the isoscalar channel (cf. also Table II). Also, in this case, the dominant neutron configurations for the PDS are $3s_{1/2} \rightarrow 3p_{3/2}$, $2d_{3/2} \rightarrow 3p_{1/2}$, $3s_{1/2} \rightarrow 3p_{1/2}$, and $2d_{3/2} \rightarrow 3p_{3/2}$ (positive sign for the partial transition amplitude), but here, the contributions from $1h_{11/2} \rightarrow 1i_{13/2}$ and $1g_{7/2} \rightarrow 1h_{9/2}$ are also positive even though an order of magnitude smaller. Because most neutron configurations add coherently to the reduced transition amplitude, the total neutron amplitude $\approx 84\text{fm}^3$ is much larger than the corresponding proton contribution $\approx 17\text{fm}^3$. In the response to the isoscalar dipole operator, all major neutron and proton partial transition amplitudes for the PDS state at 7.81 MeV are of the same sign, and this coherence leads to the large $B(E1)$ value shown in Fig. 1.

We have verified that similar results are also obtained with the other effective interactions used in this paper. Tables I and II list the dominant partially reduced transition amplitudes for the PDS in the isovector and isoscalar channels, respectively, in ^{132}Sn calculated for the five effective interactions with $a_4 = 30$, 32, 34, 36, and 38 MeV and the corresponding increasing values of the slope parameter L. In the isovector channel, both the neutron- and the proton-reduced transition amplitudes increase with a_4 and L (cf. Fig. 1). Table I shows that the contributions of the neutron and proton particle-hole configurations increase by 72% and 70%, respectively, from $a_4 = 30$, $L = 30$ MeV to $a_4 = 38$, $L = 110.8$ MeV. The increase in a_4 and L simply corresponds to an enhancement of the restoring force for isovector oscillations. However,

TABLE II. Same as described in the caption for Table I but for the partial isoscalar-reduced transition amplitudes $A_{\rm ph}^{T=0}(E1)$ with magnitudes larger than about 1fm^3.

a_4(MeV)	Config.	30	32	34	36	38
E(MeV)		7.94	7.81	7.71	7.67	7.62
				$A_{\rm ph}^{T=0}$(fm^3)		
Neutron	$3s_{1/2} \rightarrow 3p_{3/2}$	33.43	32.96	32.45	31.75	31.18
	$2d_{3/2} \rightarrow 3p_{1/2}$	12.85	14.13	15.08	15.98	16.48
	$3s_{1/2} \rightarrow 3p_{1/2}$	9.10	8.72	8.11	7.87	7.75
	$2d_{3/2} \rightarrow 3p_{3/2}$	7.11	7.73	8.41	8.75	8.78
	$1g_{7/2} \rightarrow 1h_{9/2}$	3.86	3.72	3.51	3.46	3.43
	$1h_{11/2} \rightarrow 1i_{13/2}$	3.24	2.88	2.45	2.27	2.18
	$2d_{5/2} \rightarrow 3p_{3/2}$	1.92	2.60	3.07	3.78	4.34
	$1h_{11/2} \rightarrow 3i_{13/2}$	1.18	1.32	1.41	1.57	1.69
	$2d_{5/2} \rightarrow 2f_{7/2}$	−1.16	−1.10	−1.11	−0.86	−0.57
	$1g_{7/2} \rightarrow 2f_{5/2}$	0.84	1.12	1.33	1.77	2.23
	$1h_{11/2} \rightarrow 2g_{9/2}$	0.61	1.08	1.45	2.06	2.60
	$1h_{11/2} \rightarrow 2i_{13/2}$	0.81	0.91	0.98	1.08	1.15
n total		79.70	83.89	86.29	90.76	94.31
Proton	$1g_{9/2} \rightarrow 1h_{11/2}$	5.36	6.19	6.68	7.73	8.74
	$1f_{5/2} \rightarrow 1g_{7/2}$	3.32	3.82	4.11	4.76	5.38
p total		15.69	16.95	17.83	19.89	21.77

because of the partial cancellation of proton and neutron transition amplitudes, the isovector $B(E1)$ of the PDS is generally small for all values of a_4 and L. The occurrence and evolution of strength of the PDS have been associated with the neutron excess. The correlation between neutron-skin thickness and the parameters a_4 and L has been studied using a variety of nonrelativistic and relativistic mean-field models [9,66,67]. It has been shown that, for a given nucleus, the thickness of the neutron skin increases linearly with a_4 and L. In fact, using the same set of effective interactions, in Ref. [9], we have calculated the increase in the neutron skin in ^{132}Sn from $r_n - r_p = 0.19$ fm for $a_4 = 30$, $L = 30$ MeV to $r_n - r_p = 0.36$ fm for $a_4 = 38$, $L = 110.8$ MeV. A number of papers, including the present, have shown that the strength of the pygmy state in the isovector response is enhanced with increasing a_4 and L, and this enhancement has been correlated with the corresponding increase in the neutron-skin thickness.

The situation is different in the isoscalar response. In this case, the increase in the total proton transition amplitude between $a_4 = 30$, $L = 30$ MeV and $a_4 = 38$, $L = 110.8$ MeV(39%) is much larger than that of the neutron transition amplitude (18%). However, the total contribution of proton configurations to the overall amplitude is small, varying from 16% for $a_4 = 30$, $L = 30$ MeV to 19% for $a_4 = 38$, $L = 110.8$ MeV. The structure of the PDS in the isoscalar response is, therefore, dominated by a relatively large number of neutron particle-hole configurations that, together with proton configurations, add coherently to build a reduced transition probability of collective strength.

IV. SUMMARY

In conclusion, we have employed the fully self-consistent RPA, based on the framework of relativistic energy density functionals, to analyze the isovector and isoscalar dipole responses in ^{68}Ni, ^{132}Sn, and ^{208}Pb. In particular, the evolution of PDSs in the region of low excitation energies has been analyzed as a function of the density dependence of the symmetry energy for a set of relativistic effective interactions. These interactions, adjusted to empirical properties of nuclear matter, binding energies, and charge radii of ten spherical nuclei, principally differ in their isovector properties. They span a broad range of values of the two parameters that determine the density dependence of the symmetry energy in nuclear matter: the symmetry energy at saturation density a_4 and the slope parameter L proportional to the first derivative of the symmetry energy at saturation.

The present paper confirms recent results obtained in the framework of nonrelativistic and relativistic mean-field plus RPA models [23,28,43]: (i) The range of values of the slope parameter L constrained by the measured electric dipole polarizability of ^{208}Pb [20] is consistent with the values deduced from the percentage of EWSR associated with the PDSs in ^{68}Ni [15] and ^{132}Sn [9]; (ii) the occurrence of the PDSs is predicted in the response to both the isovector and the isoscalar dipole operators, and their strength is enhanced with the increase in a_4 and L; (iii) in both channels, the PDSs exhaust a relatively small fraction of the EWSR but a much larger percentage of the inverse energy-weighted sum rule (m_{-1} moment of the strength distribution): $\approx$20% in the isovector channel and more than 50% in the isoscalar channel; (iv) for the isovector dipole operator, the reduced transition probability $B(E1)$ of the PDS is generally small because of pronounced cancellation of proton and neutron particle-hole contributions to the reduced transition amplitude; (v) the isoscalar-reduced transition amplitude is predominantly determined by neutron particle-hole configurations, most of them add coherently and, together with proton contributions, this results in a collective response of the PDS to the isoscalar dipole operator; in contrast to the result reported in Ref. [28], we find that the excitation energy of the PDS actually decreases with the systematic increase in a_4 and L, consistent with the behavior of the corresponding IVGDR.

The study in Ref. [28], performed with the Skyrme HF + RPA model as well as the present more systematic analysis based on a set of relativistic effective interactions have shown that the PDS is much more pronounced in the response to the isoscalar dipole operator and can be considered as a resonance state only in the isoscalar channel. This result indicates that isoscalar probes might be a more appropriate tool for experimental studies on pygmy dipole states in neutron-rich nuclei [14,17,25,68].

ACKNOWLEDGMENTS

This work was supported by the MZOS—Project No. 1191005-1010 and the Croatian Science Foundation as well as the Major State 973 Program No. 2007CB815000, the National Natural Science Foundation of China under Grants No. 10975008 and No. 11175002, and the Research Fund for the Doctoral Program of Higher Education under Grant No. 20110001110087 in China.

[1] N. Paar, D. Vretenar, E. Khan, and G. Colò, Rep. Prog. Phys. **70**, 691 (2007).
[2] N. Paar, J. Phys. G **37**, 064014 (2010).
[3] N. Ryezayeva, T. Hartmann, Y. Kalmykov, H. Lenske, P. von Neumann-Cosel, V. Y. Ponomarev, A. Richter, A. Shevchenko, S. Volz, and J. Wambach, Phys. Rev. Lett. **89**, 272502 (2002).
[4] A. Zilges *et al.*, Phys. Lett. B **542**, 43 (2002).
[5] T. Hartmann, M. Babilon, S. Kamerdzhiev, E. Litvinova, D. Savran, S. Volz, and A. Zilges, Phys. Rev. Lett. **93**, 192501 (2004).
[6] P. Adrich *et al.* (LAND-FRS Collaboration), Phys. Rev. Lett. **95**, 132501 (2005).
[7] D. Savran, M. Babilon, A. M. van den Berg, M. N. Harakeh, J. Hasper, A. Matic, H. J. Wörtche, and A. Zilges, Phys. Rev. Lett. **97**, 172502 (2006).
[8] S. Volz, N. Tsoneva, M. Babilon, M. Elvers, J. Hasper, R.-D. Herzberg, H. Lenske, K. Lindenberg, D. Savran, and A. Zilges, Nucl. Phys. A **779**, 1 (2006).
[9] A. Klimkiewicz *et al.* (LAND Collaboration), Phys. Rev. C **76**, 051603 (2007).

[10] A. Klimkiewicz *et al.*, Nucl. Phys. A **788**, 145 (2007).
[11] B. Özel, J. Enders, P. von Neumann-Cosel, I. Poltoratska, A. Richter, D. Savran, S. Volz, and A. Zilges, Nucl. Phys. A **788**, 385 (2007).
[12] D. Savran, M. Fritzsche, J. Hasper, K. Lindenberg, S. Müller, V. Yu. Ponomarev, K. Sonnabend, and A. Zilges, Phys. Rev. Lett. **100**, 232501 (2008).
[13] R. Schwengner *et al.*, Phys. Rev. C **78**, 064314 (2008).
[14] J. Endres, D. Savran, A. M. van den Berg, P. Dendooven, M. Fritzsche, M. N. Harakeh, J. Hasper, H. J. Wörtche, and A. Zilges, Phys. Rev. C **80**, 034302 (2009).
[15] O. Wieland *et al.*, Phys. Rev. Lett. **102**, 092502 (2009).
[16] A. P. Tonchev, S. L. Hammond, J. H. Kelley, E. Kwan, H. Lenske, G. Rusev, W. Tornow, and N. Tsoneva, Phys. Rev. Lett. **104**, 072501 (2010).
[17] J. Endres *et al.*, Phys. Rev. Lett. **105**, 212503 (2010).
[18] D. Savran *et al.*, Phys. Rev. C **84**, 024326 (2011).
[19] J. Isaak *et al.*, Phys. Rev. C **83**, 034304 (2011).
[20] A. Tamii *et al.*, Phys. Rev. Lett. **107**, 062502 (2011).
[21] S. Péru, J. F. Berger and P. F. Bortignon, Eur. Phys. J. A **26**, 25 (2005).
[22] E. G. Lanza, F. Catara, D. Gambacurta, M. V. Andrés, and Ph. Chomaz, Phys. Rev. C **79**, 054615 (2009).
[23] A. Carbone, G. Colò, A. Bracco, L.-G. Cao, P. F. Bortignon, F. Camera, and O. Wieland, Phys. Rev. C **81**, 041301 (2010).
[24] P.-G. Reinhard and W. Nazarewicz, Phys. Rev. C **81**, 051303 (2010).
[25] E. G. Lanza, A. Vitturi, M. V. Andrés, F. Catara, and D. Gambacurta, Phys. Rev. C **84**, 064602 (2011).
[26] T. Inakura, T. Nakatsukasa, and K. Yabana, Phys. Rev. C **84**, 021302 (2011).
[27] E. Yüksel, E. Khan, and K. Bozkurt, Nucl. Phys. A **877**, 35 (2012).
[28] X. Roca-Maza, G. Pozzi, M. Brenna, K. Mizuyama, and G. Colò, Phys. Rev. C **85**, 024601 (2012).
[29] P. Papakonstantinou, V. Y. Ponomarev, R. Roth, J. Wambach, Eur. Phys. J. A **47**, 14 (2011).
[30] M. Matsuo, K. Mizuyama, and Y. Serizawa, Phys. Rev. C **71**, 064326 (2005).
[31] J. Terasaki and J. Engel, Phys. Rev. C **74**, 044301 (2006).
[32] Kenichi Yoshida and Nguyen Van Giai, Phys. Rev. C **78**, 064316 (2008).
[33] J. Li, G. Colo, and J. Meng, Phys. Rev. C **78**, 064304 (2008).
[34] K. Yoshida, Phys. Rev. C **79**, 054303 (2009).
[35] S. Ebata, T. Nakatsukasa, T. Inakura, K. Yoshida, Y. Hashimoto, and K. Yabana, Phys. Rev. C **82**, 034306 (2010).
[36] M. Martini, S. Peru, and M. Dupuis, Phys. Rev. C **83**, 034309 (2011).
[37] D. Sarchi, P. F. Bortignon, and G. Coló, Phys. Lett. B **601**, 27 (2004).
[38] N. Tsoneva and H. Lenske, Phys. Rev. C **77**, 024321 (2008).
[39] D. Gambacurta, M. Grasso, and F. Catara, Phys. Rev. C **84**, 034301 (2011).
[40] J. Piekarewicz, Phys. Rev. C **73**, 044325 (2006).
[41] J. Liang, L. G. Cao, and Z. Y. Ma, Phys. Rev. C **75**, 054320 (2007).
[42] H. Liang, N. Van Giai, and J. Meng, Phys. Rev. Lett. **101**, 122502 (2008).
[43] J. Piekarewicz, Phys. Rev. C **83**, 034319 (2011).
[44] N. Paar, T. Nikšić, D. Vretenar, and P. Ring, Phys. Lett. B **606**, 288 (2005).
[45] N. Paar, Y. F. Niu, D. Vretenar, and J. Meng, Phys. Rev. Lett. **103**, 032502 (2009).
[46] D. Peña Arteaga, E. Khan, and P. Ring, Phys. Rev. C **79**, 034311 (2009).
[47] I. Daoutidis and S. Goriely, Phys. Rev. C **84**, 027301 (2011).
[48] E. Litvinova, P. Ring, and D. Vretenar, Phys. Lett. B **647**, 111 (2007).
[49] E. Litvinova, P. Ring, and V. Tselyaev, Phys. Rev. C **78**, 014312 (2008).
[50] E. Litvinova, P. Ring, V. Tselyaev, and K. Langanke, Phys. Rev. C **79**, 054312 (2009).
[51] E. Litvinova, P. Ring, and V. Tselyaev, Phys. Rev. Lett. **105**, 022502 (2010).
[52] Michael Urban, Phys. Rev. C **85**, 034322 (2012).
[53] V. Baran, B. Frecus, M. Colonna, and M. Di Toro, arXiv:1111.6504v2.
[54] R. Michaels *et al.*, Jefferson Laboratory Report No. 29, 2005 (unpublished); S. Abrahamyan *et al.* (PREX Collaboration), Phys. Rev. Lett. **108**, 112502 (2012).
[55] T. Nikšić, D. Vretenar, and P. Ring, Phys. Rev. C **66**, 064302 (2002).
[56] T. Nikšić, D. Vretenar, P. Finelli, and P. Ring, Phys. Rev. C **66**, 024306 (2002).
[57] G. A. Lalazissis, T. Nikšić, D. Vretenar, and P. Ring, Phys. Rev. C **71**, 024312 (2005).
[58] D. Vretenar, A. Wandelt, and P. Ring, Phys. Lett. B **487**, 334 (2000).
[59] D. Vretenar, T. Nikšić, and P. Ring, Phys. Rev. C **68**, 024310 (2003).
[60] P.-G. Reinhard, Nucl. Phys. A **649**, 305c (1999).
[61] G. Colò, N. Van Giai, P. F. Bortignon, and M. R. Quaglia, Phys. Lett. B **485**, 362 (2000).
[62] N. Paar, D. Vretenar, T. Nikšić, and P. Ring, Phys. Rev. C **74**, 037303 (2006).
[63] S. I. Bastrukov, S. Misicu, and V. I. Sushkov, Nucl. Phys. A **562**, 191 (1993).
[64] S. Misicu, Phys. Rev. C **73**, 024301 (2006).
[65] D. Vretenar, N. Paar, P. Ring, and T. Nikšić, Phys. Rev. C **65**, 021301(R) (2002).
[66] R. J. Furnstahl, Nucl. Phys. A **706**, 85 (2002).
[67] L. W. Chen, C. M. Ko, and B. A. Li, Phys. Rev. C **72**, 064309 (2005).
[68] A. Vitturi, E. G. Lanza, M. V. Andres, F. Catara, and D. Gambacurta, Pramana J. Phys. **75**, 73 (2010).